

Algorithm Theoretical Basis Document for Normalized Difference Vegetation Index version 2

PRODUCTS: LSA-420 AND LSA-454 (ENDVI10, 2014 - 2019)



Reference Number:
Issue/Revision Index:
Last Change:

SAF/LAND/VITO/ATBD_ENDVI10/2.3
Issue 2
26/11/2020

DOCUMENT SIGNATURE TABLE

	Name	Date	Signature
Prepared by:	E. Wolters, C. Toté, E. Swinnen	26/11/2020	
Approved by:	Land SAF Project Manager (I. Trigo)	26/11/2020	

DOCUMENTATION CHANGE RECORD

Issue / Revision	Date	Description:
Version 2.1	13/10/2017	<ul style="list-style-type: none"> Added information on the EUMETSAT PMAp AOT product (algorithm description, spatial resolution). Included summary of PMAp validation from Metzger et al. (2016). Included AOT, TOC reflectance, and TOC NDVI comparison using MetOp-B L2 TOA reflectances for latitudinal function, CAMS NRT, CAMS climatology, and PMAp.
Version 2.2	19/01/2018	Modifications following the PCR.
Version 2.3	12/11/2019	<ul style="list-style-type: none"> Replaced AOT input description from Version 2.2 with description of 10-daily AOT climatology based on CAMS re-analysis data 2003 – 2017
	26/11/2020	<ul style="list-style-type: none"> Modifications based on the ORR/DRR review comments

Table of Contents

DOCUMENT SIGNATURE TABLE.....	2
DOCUMENTATION CHANGE RECORD.....	2
1. Introduction	7
2. Input Data	10
2.1. MetOp-AVHRR	10
2.2. Meteorological data.....	11
3. Atmospheric correction	13
3.1. Introduction	13
3.2. Copernicus Atmospheric Monitoring Service (CAMS) re-analysis data	13
3.3. AOT climatology data methodology	13
3.4. SMAC limitations and AOT input constraints.....	14
3.5. Segment Processing	17
3.6. Compositing	18
3.7. LST Calculation	19
4. Product Characteristics	22
5. Quality.....	24
6. References	25

List of Tables

Table 1: Product Requirements for ENDVI10, in terms of area coverage, resolution, and accuracy.	8
Table 2: MetOp-AVHRR spectral bands.	11
Table 3: Maximum allowed AOT (AOT_{max}) to preserve positive MetOp-B-AVHRR $RED_{TOC} > 0$ for $RED_{TOA} = 0.03 - 0.10$ at $SZA = 25^\circ$ (middle column) and $SZA = 75^\circ$ (right column). The first AOT_{max} value indicates the value at $VZA = 0^\circ$, whereas the second value is the AOT_{max} at $VZA = SZA + 60^\circ$	16
Table 4: Compositing rules.	19
Table 5: Image layers comprised in each 10-daily composite of METOP-AVHRR (ENDVI10).	22
Table 6: Bit-interpretation of the Status Map (Bit7=Most Significant Bit, MSB).	23

List of Figures

Figure 1: ENDVI10 product example.	7
Figure 2: SMAC MetOp-B RED_{TOC} reflectance calculations for $RED_{TOA} = 0.03, 0.06, \text{ and } 0.09$ and for fixed $SZA=25^\circ$ (left column) and $SZA=75^\circ$ (right column). RED_{TOC} is plotted as function of the joint viewing and solar zenith angles ($SZA+VZA$, y axis) and AOT (x axis). RED_{TOC} is indicated by red colours as positive, which gradually change towards white for near-zero values and finally into blue colours for negative RED_{TOC}	15

List of Acronyms

AL	Albedo Product
AOT	Aerosol Optical Depth
ASCAT	Advanced Scatterometer
ATBD	Algorithm Theoretical Baseline Document
AVHRR	Advanced Very High Resolution Radiometer
BT	Brightness Temperature
CAMS	Copernicus Atmosphere Monitoring Service
CDR	Climate Data Record
EARS	EUMETSAT Advanced Retransmission Service
EC	European Commission
ECMWF	European Centre for Mid-Range Weather Forecasts
ENDVI	EPS NDVI
EPS	EUMETSAT Polar System
EP-TOMS	Earth Probe - Total Ozone Monitoring Spectrometer
EUMETSAT	European Organisation for the Exploitation of Meteorological Satellites
GLSDEM	Global Land Survey Digital Elevation Model
ICDR	Intermediate Climate Data Record
IFS	Integrated Forecasting System
IPMA	Instituto Português do Mar e da Atmosfera
JRC	Joint Research Centre
LSA SAF	Land Surface Analysis Satellite Application Facility
LST	Land Surface Temperature
LT	Local Time
MACC-II	Monitoring Atmospheric Composition and Climate – Interim Implementation

MARS	Monitoring Agricultural Resources
MBE	Mean Bias Error
MetOp	Meteorological Operational Satellites
MIR	Medium Infrared
MODIS	Moderate Resolution Imaging Spectroradiometer
NDVI	Normalised Difference Vegetation Index
NIR	Near Infrared
NOAA	National Oceanic and Aeronautic Administration
NRT	Near Real Time
NWP	Numerical Weather Prediction
PDU	Product Dissemination Unit
PRD	Product Requirements Document
RMSE	Root Mean Squared Error
SAA	Solar Azimuth Angle
STM	Status Map
SMAC	Simplified Method for Atmospheric Correction
SPOT-VEGETATION	Satellite Pour l'Observation de la Terre - Végétation
SR	Surface Reflectance
SW	Shortwave
SWIR	Shortwave Infrared
SZA	Solar Zenith Angle
TIR	Thermal Infrared
TOA	Top-Of-Atmosphere
TOC	Top-Of-Canopy
UMARF	Unified Meteorological Archive and Retrieval
VAA	Viewing Azimuth Angle
VITO	Flemish Institute for Technological Research

VZA

Viewing Zenith Angle

WGS84

World Geodetic System 1984

1. Introduction

The Satellite Application Facility (SAF) on Land Surface Analysis (LSA) is part of the SAF Network, a set of specialized development and processing centres, serving as EUMETSAT (European Organization for the Exploitation of Meteorological Satellites) distributed Applications Ground Segment. The SAF network complements the product-oriented activities at the EUMETSAT Central Facility in Darmstadt. The main purpose of the LSA SAF is to take full advantage of remotely sensed data, particularly those available from EUMETSAT sensors, and to measure land surface variables, which will find primarily applications in meteorology (<http://landsaf.ipma.pt/>).

The EUMETSAT Polar System (EPS) is Europe's first polar orbiting operational meteorological satellite system and the European contribution to a joint polar system with the USA. EUMETSAT has the operational responsibility for the "morning orbit" with Meteorological-Operational (MetOp) satellites, the first of which (MetOp-A) was successfully launched on 19 October 2006 and the second (MetOp-B) launched on 17 September 2012. The third MetOp satellite (MetOp-C) was launched on 7 November 2018 and became operational on 3 July 2019. Despite the wide range of sensors on-board MetOp (<http://www.eumetsat.int/>), most LSA SAF parameters make use of the Advanced Very High Resolution Radiometer (AVHRR) and, to a lesser extent, of the Advanced Scatterometer (ASCAT).

The MetOp-AVHRR S10 EPS Normalised Difference Vegetation Index (ENDVI) data are near-global, 10-daily composite images which are synthesized from the "best available" observations registered per dekad (10-day period) by the orbiting earth observation instrument MetOp-AVHRR, as shown in a yearly composite of 2009 in Figure 1.

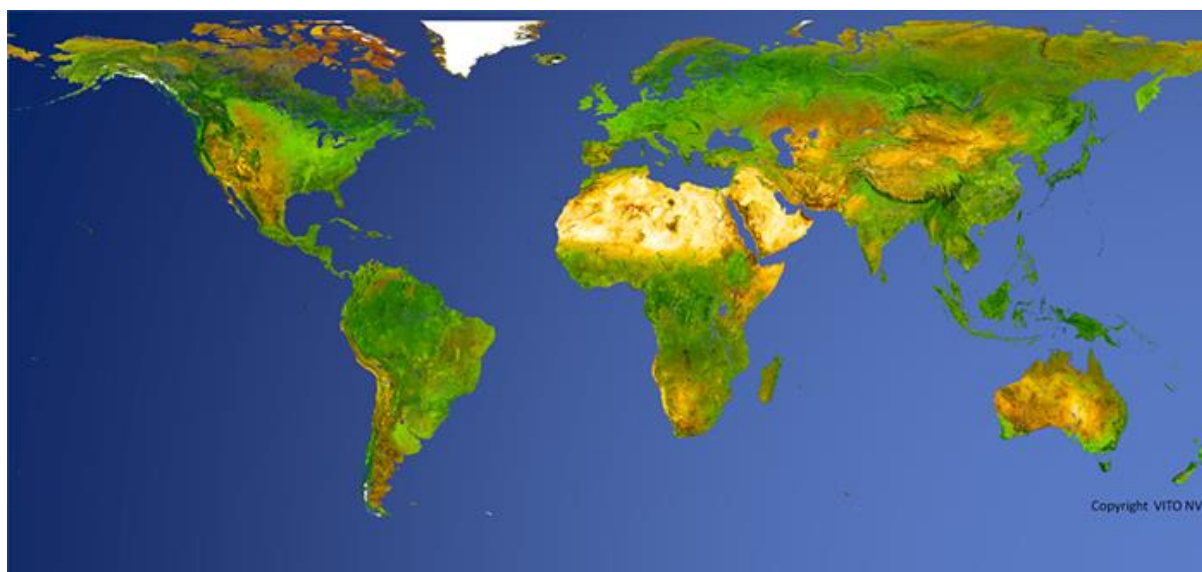


Figure 1: ENDVI10 product example.

On behalf of the Joint Research Centre – Monitoring Agricultural Resources (JRC-MARS) program of the European Commission (EC), the Flemish Institute for Technological Research (VITO) has developed a NOAA-AVHRR data processing chain over Europe. Individual tracks/orbits are ingested, corrected in different steps (calibration, geometric correction, atmospheric correction, cloud/snow labelling, etc.) and then composited to 10-daily synthesis images (S10). With this chain, all daytime-observed NOAA data registered since 1981 were processed by different research institutes in Europe. The procedures were adapted for MetOp-AVHRR Level 1b data. The resulting MetOp-AVHRR S10 composites are very comparable with those delivered by VITO's SPOT-VEGETATION processing chain: 1 km resolution, near-global daily coverage, a 10-day frequency ("dekad"), and similar spectral characteristics: RED (0.58 - 0.68 μm), Near Infrared (NIR, 0.725 - 1.00 μm), Shortwave Infrared (SWIR, 1.58 - 1.64 μm) - no BLUE, but two Thermal Infrared (TIR) bands. In addition to the basic image layers (surface reflectances, solar and viewing geometry angles, status map, etc.), the dekad composites also comprise two "value-added" image layers: NDVI and Land Surface Temperature (LST).

The MetOp-AVHRR S10 is operated in the LSA SAF System II at VITO. The ENDVI10 is available as a Climate Data Record (LSA-454), starting in March 2007, and as an Interim Climate Data Record (LSA-420), providing continuous Near Real Time (NRT) updates of LSA-454. At present (November 2019), the dataset spans the AVHRR sensor on-board the MetOp-A, -B, and -C satellites. For both datasets, the ENDVI10 consists of composites representing an NDVI and is distributed together with a set of ancillary datasets (surface reflectances for the RED – SWIR bands, solar and viewing zenith angles, and quality indicators). The NDVI is calculated from the AVHRR RED and NIR atmospherically corrected spectral surface reflectances as follows:

$$NDVI_{TOC} = \frac{(NIR_{TOC} - RED_{TOC})}{(NIR_{TOC} + RED_{TOC})} \quad (\text{Eq. 1})$$

The product and ancillary datasets described in this document refer to both LSA SAF products: the ENDVI10 CDR (LSA-454) and ENDVI10 ICDR (LSA-420). The LST ancillary dataset is added on courtesy of VITO, whereof EUMETSAT does not take any liability, responsibility, and ownership. The products can be acquired from <http://landsaf.ipma.pt>. An overview of the ENDVI10 Product Requirements is given in Table 1.

This document describes the algorithm and main characteristics of the vegetation index (NDVI plus accompanying spectral band reflectances and LST) generated from MetOp-AVHRR observations. The characteristics of AVHRR-based vegetation indices provided by the LSA SAF are described in the Product User Manual (PUM). Further details on the LSA SAF product requirements can be found in the Product Requirements Document (PRD), available at the LSA SAF website <http://landsaf.ipma.pt>.

Because the algorithm is based on NOAA-AVHRR data, several algorithm parts are described within this context and describe the adaptations required to support the METOP-AVHRR system.

Table 1: Product Requirements for ENDVI10, in terms of area coverage, resolution, and accuracy.

Product Name	Product Identifier	Coverage	Resolution	Accuracy
--------------	--------------------	----------	------------	----------

			Temporal	Spatial	Threshold	Target	Optimal
ENDVI10	LSA-454 LSA-420	Global	10-daily	1 km	$R^2 > 0.80$	$R^2 > 0.90$	$R^2 > 0.95$

where R^2 = coefficient of determination (explained variance).

The coefficient of determination (R^2) indicates the agreement or covariation between two datasets with respect to a linear regression model. It summarizes the total data variation explained by this linear regression model. The result varies between 0 and 1, with higher R^2 values indicating higher covariation between the datasets. In order to detect a systematic difference between the two datasets, the regression line coefficients should be used. A disadvantage of using R^2 is that it only measures the strength of the relationship between the data, but gives no indication when the data series have similar magnitude (Duveiller et al., 2016a).

$$R^2 = \left(\frac{\sigma(X,Y)}{\sigma(X) \cdot \sigma(Y)} \right)^2 \quad (\text{Eq. 2})$$

with $\sigma(X)$ and $\sigma(Y)$ the X and Y standard deviation and $\sigma(X,Y)$ the X and Y covariation, respectively. The R^2 is only provided together with the regression analysis in the global statistical analysis (see below), because it allows for a quantitative interpretation of the scatterplots.

2. Input Data

2.1. MetOp-AVHRR

The 1 km resolution image data registered globally by MetOp-AVHRR are systematically downlinked to the receiving station on Svalbard (Norway, 78.23°N, 15.41°N) and further channelled to EUMETSAT (Darmstadt, Germany). EUMETSAT immediately applies some crucial pre-processing steps: the raw observations are calibrated and transformed into top-of-atmosphere radiances (TOA), accurate “Lon/Lat-planes” are added with the geographical position of each pixel in the raw segment, and also a mask indicating the status of each observation (clear, cloud, snow) is added. The resulting data stream is cut into 3-minute segments (1080 scanlines), which are distributed in Near Real Time via the EUMETCast broadcasting system as EPS-formatted Level1b files.

While MetOp follows a "morning orbit", with daytime registrations in the descending node, the NOAA18 satellite oppositely has an afternoon orbit, with daytime scanning in ascending node. Both platforms carry the same AVHRR/3 sensor, but the one on-board MetOp has some advanced features. First, the satellite's orbit is better stabilised and attitude variations are limited, which benefits the geometric correction. Second, MetOp stores all last orbit's 1 km data on board – such that Darmstadt receives global 1 km imagery. EUMETSAT collects the data, pre-processes them to a basic level (Level 1B) and transmits the results freely via the EUMETCast Advanced Retransmission Service (EARS) system.

For MetOp-AVHRR, the data are cut into 3-minute segments (1080 scanlines) and distributed via the so-called EPS format. The three important differences with NOAA/AVHRR are:

- The MetOp data are global.
- The short-wave spectral calibration is already executed by EUMETSAT, hence the EPS files contain TOA radiances.
- The Lon/Lat-planes are computed by EUMETSAT and stored inside the EPS files.

Missing MetOp-AVHRR data can be ordered via the Unified Meteorological Archive and Retrieval (UMARF) system in EPS format.

The AVHRR/3 sensor on-board MetOp registers in five spectral bands, as is shown in Table 2. During daytime, Band 3 observes in the SWIR (3A), whereas during night-time it is switched to the Medium Infrared (MIR, Band 3B).

Table 2: MetOp-AVHRR spectral bands.

Band nr.	Bandwidth (μm)	Spectral domain	Band abbreviation
1	0.58 - 0.68	Shortwave	VIS (visual) or RED
2	0.725 - 1.00	Shortwave	NIR (near infrared)
3A	1.58 - 1.64	Shortwave	SWIR (shortwave infrared)
3B	3.55 - 3.93	Medium Infrared	MIR
4	10.3 - 11.3	Thermal Infrared	TIR ₄
5	11.5 - 12.5	Thermal Infrared	TIR ₅

The Level1b files are provided with a timeliness of 2 h 15 minutes from sensing with a Product Dissemination Unit (PDU) of 3 minutes, the latter also known as a product ‘granule’. These granules follow a file naming convention:

`<instrument_id>_<product_type>_<processing_level>_<spacecraft_id>_
<sensing_start>_<sensing_end>_<processing_mode>_<disposition_mode>_<processing_time>`

, so an example is

AVHR_xxx_1B_M02_20190630223103Z_20190701001303Z_N_O_20190701000922Z.nat,
which indicates that the Metop-A (M02) Level 1B data were acquired from 30 June 22:31:03 UTC to 1 July 2019 00:13:03 UTC and were processed at 1 July 2019, 00:09:22 UTC.

The EPS segments always provide the longitude and latitude on the WGS84 geodetic datum for a subsample of pixels. The WGS84 geodetic datum is the global standard for geographical projections. It comprises an ellipsoid with a semi-major and a semi-minor axis of 6,378,137 m and 6,356,752.315 m, respectively, and an oblateness (flattening) of 0.0033528 (=1/298.25722356). These "Lon/Lat-planes" are required for the mapping of the raw images towards a geographical projection system.

2.2. Meteorological data

Meteorological data are required to perform the Atmospheric Correction on the VIS/NIR channels and to compute the accompanying LST. The following ancillary data are used:

- Ozone content is obtained from an Earth Probe - Total Ozone Monitoring Spectrometer (EP-TOMS) climatology, from which one file per month is available. The data are considered representative for month day 15. The dataset’s resolution is $32 \times 32 \text{ km}^2$.
- Water vapor is derived from the actual ECMWF Numerical Weather Prediction Model (NWP) data (global, at $0.25^\circ \times 0.25^\circ$, every 6 hours).
- Tropospheric aerosol:
 - For ENDVI version 2, a 10-daily AOT climatology based on the Copernicus Atmospheric Monitoring Service (CAMS) re-analysis AOT data for 2003 – 2017

was generated to serve as aerosol input for the atmospheric correction (see §3.3).

In the previous version (ENDVI version 1) a simple Gaussian curve as a function of latitude was used. The AOT did not vary with longitude and time and had a resolution of $32 \times 32 \text{ km}^2$, interpolated bi-linearly to 1 km during processing.

- Pressure is calculated from the Global Land Survey Digital Elevation Model (GLSDEM) through the formula:

$$P = 1013.25 \cdot \left(1 - \frac{0.0065 \cdot h}{288.16}\right)^{5.31} \quad (\text{Eq. 3})$$

With P the pressure and h the altitude in meters. The meteorological input data is spatially interpolated to the AVHRR 1 km image resolution. The nearest input in time is always used, i.e., no temporal interpolation is applied.

3. Atmospheric correction

3.1. Introduction

In the previous version (ENDVI10 v1), the (tropospheric) Aerosol Optical Thickness required for the atmospheric correction procedure was initially approximated using a static Gaussian function solely based on the latitude of observation (Berthelot et al., 1997). This AOT approximation will be referred to as AOT_{LATCLIM} hereafter. Assuming that tropospheric aerosols are longitude- and time-invariant is physically unrealistic and thus increases the probability of an incorrect atmospheric correction and in turn incorrect TOC reflectances.

Therefore, in ENDVI10 v2 AOT information from the Copernicus Atmospheric Monitoring Service (CAMS) re-analysis was implemented. The following paragraphs provide a description of the CAMS re-analysis data (§3.2) and the methodology to derive an AOT climatology (§3.3).

3.2. Copernicus Atmospheric Monitoring Service (CAMS) re-analysis data

The CAMS re-analysis (hereafter referred to as CAMS_{CLIM}) is the latest global re-analysis data set of atmospheric composition (AC) produced by the Copernicus Atmosphere Monitoring Service, consisting of 3-dimensional time-consistent AC fields, including aerosols, chemical species and greenhouse gases, of which the latter are not included yet. CAMS_{CLIM} was produced using 4-dimensional variational data assimilation (4DVar) ECMWF's Integrated Forecast System (IFS), with 60 hybrid pressure (model) levels in the vertical, from surface up to the 0.1 hPa level (~36.6 km altitude) containing atmospheric data. An extensive suite of atmospheric components satellite retrievals are assimilated. For AOT, retrievals from Moderate Resolution Imaging Spectroradiometer (MODIS)-Aqua and -Terra, and Environmental Satellite (ENVISAT) Advanced Along-Track Scanning Radiometer (AATSR) are assimilated. More scientific and technical details can be found in Inness et al. (2019).

Generally, the CAMS_{CLIM} data are available at a sub-daily and monthly frequency and consist of analyses and 48 h forecasts, initialised daily from analyses at 00 UTC. The data are archived in the ECMWF data archive and can be retrieved using the ECMWF Public Dataset service via the WebAPI.

CAMS_{CLIM} contains various improvements to the re-analysis data of its precursor Monitoring Atmospheric Composition and Climate - Interim Implementation (MACC-II). A list of the most important improvements is given below.

- Newer model cycle (higher horizontal and vertical resolution)
- Higher temporal resolution
- Longer forecasts (48 hours) from 00:00 UTC
- Chemistry routines included in the Integrated Forecasting System (IFS)
- More chemical analysis fields available
- Newer, reprocessed satellite retrievals assimilated
- Ozone and aerosols are used interactively in radiation scheme

3.3. AOT climatology data methodology

The 10-daily AOT climatology for the atmospheric correction was generated from the CAMS_{CLIM} data, which at the time of download (July 2019) contained data covering the period 2003 – 2017.

The CAMS_{CLIM} total AOT was downloaded as monthly NetCDF files. These files contain per 3-hour time step the column-integrated AOT representative for $0.55 \mu\text{m}$ at $0.125^\circ \times 0.125^\circ$ resolution.

For each 10-day period, synchronized with the dekads for which MetOp ENDVI v2 data are generated, per CAMS grid cell all 3-hour values were collected and sorted, after which the 30th percentile was calculated. The 30th percentile choice was adopted from a daily AOT climatology based on the MACC-II re-analysis data generated by Meteo-France for their LSA SAF Surface Albedo (AL) product. However, in initial tests it was found that these daily AOT 30th percentile data frequently contain too high values to apply a proper atmospheric correction in case of high SZA/VZA for the ENDVI product, due to known limitations in the Simplified Method for Atmospheric Correction (SMAC, Rahman and Dedieu, 1994). In such cases, for example over dark vegetated surfaces at low solar elevation, the RED TOC reflectance obtained from SMAC can become either negative or only very slightly positive, which consequently leads to anomalously high NDVI values. Therefore an assessment on the SMAC limitations in terms of AOT, SZA, VZA, and RED TOA reflectances was performed to set up AOT input constraints before SMAC is applied.

3.4. SMAC limitations and AOT input constraints

SMAC is a very fast atmospheric correction algorithm and is used in various operational satellite surface reflectance processing chains. However, its simplifications result in a decreasing accuracy in case of high aerosol load (typically $> \sim 0.5$), especially in combination with large SZA and/or VZA. These limitations were particularly stressed by Proud et al. (2010), in which the SMAC accuracy for Meteosat-SEVIRI short-wave TOC reflectances were assessed against values obtained from Second Simulation of a Satellite Signal in the Solar Spectrum (6SV). It was shown that for joint SZA+VZA exceeding $\sim 60^\circ$ the SMAC atmospheric correction significantly starts to decrease, especially for cases with moderate to high water vapor ($> 2 \text{ g cm}^{-2}$) and/or ozone load ($> \sim 0.25 \text{ atm.cm}$).

In order to define the SMAC AOT limitations for MetOp-AVHRR, RED_{TOC} reflectances were simulated for a range of AOT, RED_{TOA} reflectances, SZA, and VZA values. These simulations were performed for MetOp-B-AVHRR, thereby assuming that the results for MetOp-A and -C would not significantly deviate, given the small differences in the MetOp-A – C spectral responses.

The RED_{TOA} reflectances ranged between 0.03 and 0.10 in steps of 0.01. Simulations were performed for SZA of 25° and 75° , being the observed global minimum and maximum MetOp values throughout the year. RED_{TOC} reflectances were obtained for joint SZA+VZA ranging from the actual SZA up to a value of SZA + 60° . Total Column Water Vapor (TCWV) and ozone concentration values were fixed at 2 g cm^{-2} and 0.300 atm.cm (300 Dobson Units), respectively.

Examples of transects through these simulations for RED_{TOA} reflectances of 0.03, 0.06, and 0.09 are shown in Figure 2. The left and right columns present results for SZA = 25° and SZA = 75° , respectively. Positive RED_{TOC} reflectances are indicated in red colors, while (physically impossible) negative values are indicated in blue colors. Values around zero are indicated in white. It can be seen that for all simulations, the maximum AOT decreases with increasing SZA+VZA. In addition, the maximum AOT decreases for decreasing RED_{TOA} reflectance. At SZA= 75° , the AOT range becomes very small, with AOT_{max} ~ 0.4 at RED_{TOA} = 0.09, which demonstrates the severe limitations of SMAC for these illumination conditions.

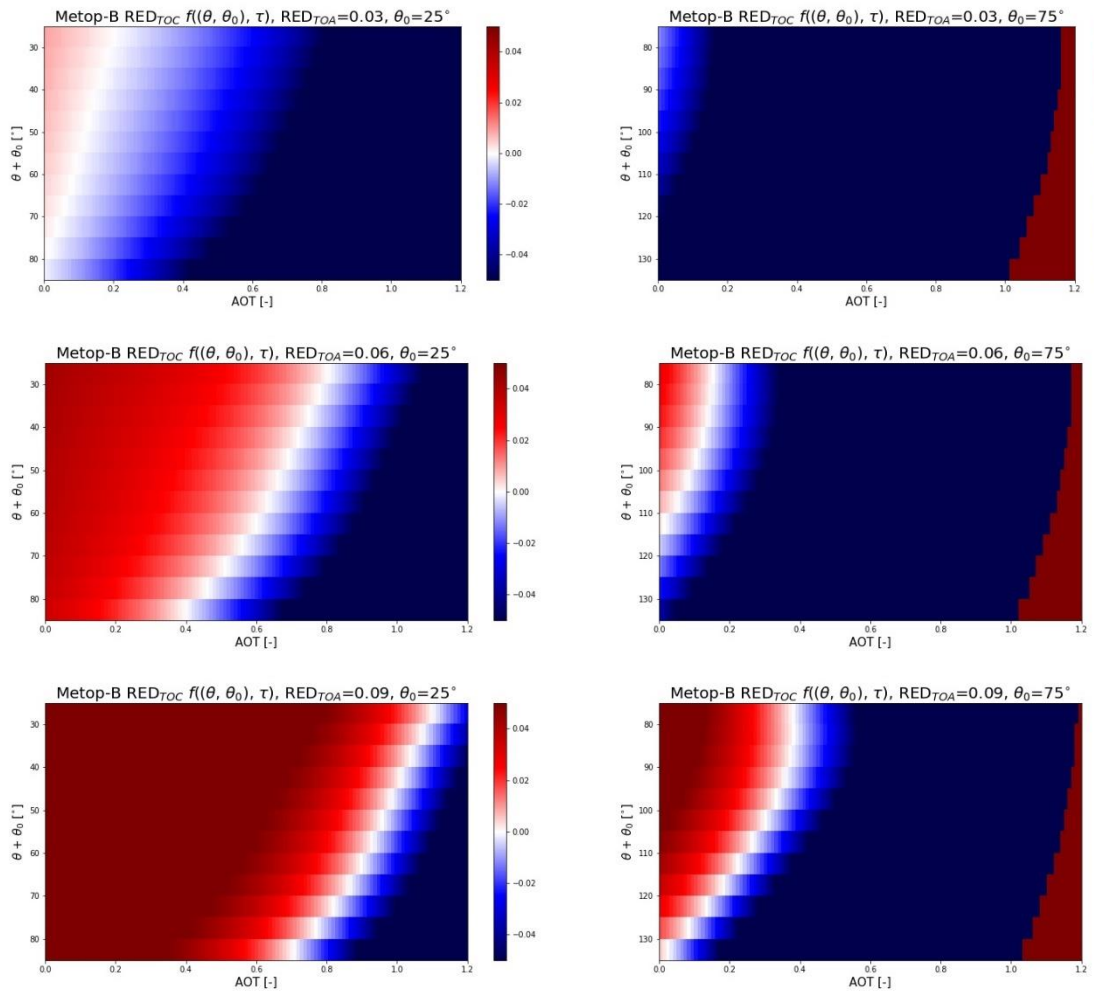


Figure 2: SMAC MetOp-B RED_{TOC} reflectance calculations for $RED_{TOA} = 0.03, 0.06,$ and 0.09 and for fixed $SZA=25^\circ$ (left column) and $SZA=75^\circ$ (right column). RED_{TOC} is plotted as function of the joint viewing and solar zenith angles ($SZA+VZA$, y axis) and AOT (x axis). RED_{TOC} is indicated by red colours as positive, which gradually change towards white for near-zero values and finally into blue colours for negative RED_{TOC} .

Subsequently, for all simulations the AOT_{max} at nadir and at $VZA= 60^\circ$ was determined for SZA values of 25° and 75° . The results are shown in Table 3.

Table 3: Maximum allowed AOT (AOT_{max}) to preserve positive MetOp-B-AVHRR $RED_{TOC} > 0$ for $RED_{TOA} = 0.03 - 0.10$ at $SZA = 25^\circ$ (middle column) and $SZA = 75^\circ$ (right column). The first AOT_{max} value indicates the value at $VZA = 0^\circ$, whereas the second value is the AOT_{max} at $VZA = SZA + 60^\circ$.

RED_{TOA}	AOT_{max} , $VZA=0^\circ$ and $VZA=60^\circ$ @ $SZA=25^\circ$	AOT_{max} , $VZA=0^\circ$ and $VZA=60^\circ$ @ $SZA=75^\circ$
0.03	0.1, 0.0	0.0
0.04	0.3, 0.1	0.0
0.05	0.5, 0.2	0.0
0.06	0.7, 0.35	0.1, 0.0
0.07	0.8, 0.45	0.15, 0.0
0.08	0.9, 0.55	0.2, 0.0
0.09	1.0, 0.65	0.25, 0.0
0.10	1.1, 0.75	0.3, 0.0

Based on the results above, two RED_{TOA} regimes were identified, $RED_{TOA} \leq 0.06$ and $RED_{TOA} > 0.06$. For both regimes, the AOT_{max} as function of RED_{TOA} , VZA , and SZA is determined in two steps. First, AOT_{max} at nadir conditions ($AOT_{max,n}$) for the actual SZA , using linear interpolation of the results for $SZA = 25^\circ$ and $SZA = 75^\circ$, is determined. Subsequently, this AOT_{max} is refined for the actual VZA , using linear interpolation of the results between $VZA=0^\circ$ and $VZA=60^\circ$. If the AOT from the 10-daily CAMS re-analysis climatology exceeds the calculated AOT_{max} , this AOT_{max} is used in the SMAC RED_{TOC} calculation, thereby preserving $RED_{TOC} > 0$.

For $RED_{TOA} \leq 0.06$, AOT_{max} is determined as follows:

$$\tau_{max,n} = \frac{\theta_{s,max} - \theta_s}{\theta_{s,max} - \theta_{s,min}} (20RED_{TOA} - 0.5) \quad (\text{Eq. 4})$$

$$\tau_{max}(\theta_v) = \tau_{max,n} - \left(\frac{\theta_v \tau_{max,n}}{60} \right) \quad (\text{Eq. 5})$$

With $\tau_{max,n}$, θ_s , and θ_v being AOT_{max} , SZA and VZA , respectively. $\theta_{s,min}$ and $\theta_{s,max}$ were set at 25° and 75° , respectively.

For $RED_{TOA} > 0.06$, the formulas to derive AOT_{max} read:

$$\tau_{max,N} = 10RED_{TOA} - (0.3 + 5RED_{TOA}) \left(\frac{\theta_s - \theta_{s,min}}{\theta_{s,max} - \theta_{s,min}} \right) + 0.1 \quad (\text{Eq. 6})$$

$$\tau_{max}(\theta_v) = \max \left[0, \tau_{max,nadir} - \left(\frac{0.35\theta_v}{60} \right) \right] \quad (\text{Eq. 7})$$

3.5. Segment Processing

The segment processing starts from AVHRR Level1B files that are received from the EUMETCast Reception Station (one base, one spare). For the ENDVI10 production, only the daytime segments are used (hence Band 3 is always SWIR).

The algorithm (Eerens et al., 2009) consists of two steps: 1) segment processing and 2) compositing.

First, each individual segment is processed as follows:

- ***Segment selection***

The continuous data stream comprises all kinds of MetOp-AVHRR imagery, registered over land and sea, during daytime and night-time. As the focus is on global vegetation monitoring, only the daytime segments that contain land pixels are selected for further processing, while sea and ocean pixels are discarded. The elimination of the night-time registrations implies that Band 3 always corresponds with the SWIR spectral range (B3A).

- ***Spatial - Remap***

Using the earlier mentioned Lon/Lat-planes, included by EUMETSAT in the Level1B EPS data, and a "nearest neighbour" resampling scheme, the five AVHRR spectral band observations are converted to the WGS84 Geographical Lon/Lat system, with a spatial resolution of $1^\circ/112$ (≈ 1 km).

- ***Spatial - Angles***

Similar images are processed to provide the solar and sensor angular position (zenith/azimuth) per pixel at the time of observation.

- ***Spectral - Shortwave***

The on-board registered TOA reflectances are converted into TOC reflectances through SMAC v4, which corrects for the atmospheric contribution to the satellite-observed (TOA) reflectance. The SMAC coefficients for MetOp-AVHRR's three shortwave channels (RED, NIR, and SWIR) were computed on behalf of the MARS project (Berthelot et al, 2008). In addition to these band-specific coefficients, SMAC also requires water vapour, ozone content, and AOT, as described in Section 2.2.

After atmospheric correction, the Normalised Difference Vegetation Index (NDVI) is computed from the surface (TOC) reflectances.

- ***Spectral - Longwave***

Land surface temperatures (LST) are derived separately for land and sea pixels from the two TIR Brightness Temperatures (BT) using the split window technique [Coll and Caselles, 1997], which also requires water vapour and TIR emissivity input. For water vapour, the same 6-hourly ECMWF data are used as for the atmospheric correction. The land TIR emissivities are computed via a simple linear equation from the NDVI. More details are provided in Section 3.7.

- **Quality - Masking**

Each pixel's observational state is expressed via 0/1 switches in a bitmap image. This status mask classifies each pixel according to criteria such as land/sea, clear/cloud, and snow/ice. While the GLC2000 map (Bartholomé et al, 2005) is used to separate land from sea pixels, the distinction between "clear/cloud/snow/ice" is fully based on the results of the cloud/snow detection added by EUMETSAT to the Level1B files (EUMETSAT, 2004).

3.6. Compositing

The processed segments are further processed into daily composites before the final 10-daily composites (S10):

- **Spatial aspects**

The composite images follow the same map system as the corrected segments, i.e., WGS84 Geographical Lon/Lat, with a resolution of 1°/112. While the segments only cover limited zones, the S10 composites always extend over the same near-global area, ranging from -180° to +180° longitude and -56° to +75° latitude (40,320 columns × 14,673 lines). The composites only contain information for the land pixels. All water pixels are flagged with unique missing values codes.

- **Temporal aspects**

Every month is divided in three "dekads". The first two always comprise ten days (1-10, 11-20), the third one has variable length, as it runs from day 21 until the end of the month. The procedure starts with the selection of all segments registered within the concerned dekad and overlapping at least partially with the mentioned target zone.

- **Spectral aspects**

In general, for each land pixel in the composite, different observations are available, from different segments or registration dates. The compositing selects the "best available" observation and transfers its components (TOC reflectances, Land Surface Temperatures, angles, status, day of observation, and number of clear observations) to the corresponding layers in the S10 synthesis. The selection is realised as follows. For each pixel, the available observations are first classified based on their status (clear, snow/ice, cloud) and their geometry (ϑ_s =SZA, ϑ_v =VZA), as shown in Table 4.

Table 4: Compositing rules.

OBSERVATION STATUS	REGISTRATION GEOMETRY		
	BAD $\theta_s > 75^\circ$ or $\theta_v > 45^\circ$	ACCEPTABLE $\theta_s < 75^\circ$ and $40^\circ < \theta_v < 45^\circ$	GOOD $\theta_s < 75^\circ$ and $\theta_v < 40^\circ$
Cloud	<i>Not used</i>	C2	C1
Snow/Ice	<i>Not used</i>	B2	B1
Clear	<i>Not used</i>	A2	A1

All observations in the BAD category are immediately discarded. The remaining ones (if any) are grouped into six classes, with the following hierarchy: $A1 > A2 > B1 > B2 > C1 > C2$.

Subsequently, the highest non-empty class is searched. If it contains only one observation, that one is selected, otherwise it will be the one with the highest NDVI (which prefers cloud-free and snow-free observations). If a pixel has no 'GOOD' or 'ACCEPTABLE' observations, its position in the composite is flagged with special codes in all spectral layers. But in all other cases (at least one acceptable measurement), the composite will contain the values of the best observation (reflectances, angles, etc.), while its nature (clear, cloudy,...) is expressed via the Status Map.

This method favours the near-nadir views and suppresses observations that are still partly affected by clouds, snow, and water (which all have low NDVI).

▪ **Quality Control**

NOAA-AVHRR scenes were often affected by radiometric errors (stripes, waves) or geometrical shifts, especially when a platform reaches its nominal lifetime. Hence, after the pre-processing each individual segment is visually checked by an operator who identifies and rejects the bad scenes. Without this measure, the bad segments can decrease the final composites' quality. However, during one year of similar checks on the AVHRR data of MetOp, no such errors could be detected. Therefore now only the daily global composites, which are produced in the background, are checked. This requires less time and is as effective as checking hundreds of individual segments (480 per day).

3.7. LST Calculation

In the LST calculation process, the fractional vegetation cover is calculated using the obtained NDVI. For each pixel, this fraction is determined using the pixels within the imagery with maximum and minimum NDVI.

The fractional vegetation cover (P_v) is calculated using the median of the pixels having the 5% highest NDVI values ($NDVI_v$) and the median of the pixels having the 5% lowest NDVI values ($NDVI_g$).

$$P_v = \frac{NDVI - NDVI_g}{NDVI_v - NDVI_g} \quad (\text{Eq. 8})$$

with:

P_v	: Vegetation fraction [-]
$NDVI$: Normalized Difference Vegetation Index of the pixel [-]
$NDVI_g$: maximum Normalized Difference Vegetation Index of a bare soil pixel [-]
$NDVI_v$: minimum Normalized Difference Vegetation Index of a fully vegetated pixel [-]

The calculation procedure consists of the following steps.

- Sort all unique pixels from the smallest to the largest value
- Select pixels with the $x\%$ (default is 5%) highest and lowest NDVI values. The median of the $x\%$ highest is $NDVI_v$ and the median of the lowest $x\%$ is $NDVI_g$;
- For each pixel, calculate P_v .

For the LST calculation, a split window method is used. The brightness temperatures (BT) from Band 4 and 5 are combined with the surface emissivity (the ratio of an object's emitted radiance to that of a perfect black body) and the atmospheric water vapour content is taken into account.

The emissivity (ϵ , [-]) is calculated according to Valor and Caselles (1996) and Rubio et al. (1997):

$$\epsilon = \epsilon_v \cdot P_v + \epsilon_g \cdot (1 - P_v) + 4 \cdot \langle d\epsilon \rangle \cdot P_v \cdot (1 - P_v) \quad (\text{Eq. 9})$$

with:

ϵ	: pixel emissivity [-]
ϵ_v	: the emissivity of a fully vegetated pixel [-]
ϵ_g	: the emissivity of a bare soil pixel [-]
$d\epsilon$: the estimated mean error on the values of ϵ_v and ϵ_g [-]

The emissivity difference ($\Delta\epsilon$) as a function of the vegetation cover fraction (P_v) is calculated as:

$$\Delta\epsilon = (\Delta\epsilon_{(P_v=1)} - \Delta\epsilon_{(P_v=0)}) \cdot P_v + \Delta\epsilon_{(P_v=0)} \quad (\text{Eq. 10})$$

with:

$\Delta\epsilon$: pixel emissivity difference between Band 4 and 5 [-]
$\Delta\epsilon_{(P_v=1)}$: the emissivity difference of a fully vegetated pixel [-]
$\Delta\epsilon_{(P_v=0)}$: the emissivity difference of a bare soil pixel [-]

Corrections for the atmospheric influence on the BT are:

$$\alpha = W^3 - 8 \cdot W^2 + 17 \cdot W + 40 \quad (\text{Eq. 11})$$

$$\beta = 150 \cdot \left(1 - \frac{W}{4.5}\right) \quad (\text{Eq. 12})$$

$$\text{offset} = \alpha \cdot (1 - \varepsilon) - \beta \cdot \Delta \varepsilon \quad (\text{Eq. 13})$$

with:

α , β and offset : corrections for emissivity and water vapour content in the atmosphere
[-]

W : the atmospheric water vapour content [g cm^{-2}], see Section 2.2.

Finally, the LST is determined according to the split-window technique (Coll and Caselles, 1997):

$$LST = BT4 + [1.34 + 0.39 \cdot (BT4 - BT5)] \cdot (BT4 - BT5) + 0.56 + \text{offset} \quad (\text{Eq. 14})$$

with:

$BT4$, $BT5$: the brightness temperatures of Band 4 and 5 [K]

4. Product Characteristics

In a spectral/thematic sense, each S10 composite comprises the 12 image layers listed in tables Table 5 and Table 6.

Table 5: Image layers comprised in each 10-daily composite of METOP-AVHRR (ENDVI10).

IMAGE		Physical Values Y			Scaling	Digital Values V	
SUF	DT	CONTENT	UNIT	$Y_{lo} \rightarrow Y_{hi}$	$Y=A+B*V$	$V_{lo} \rightarrow V_{hi}$	V_{flag}
SR1	1	$R_{s,RED}$	-	$0 \rightarrow 0.625$	$Y=0.0025*V$	$0 \rightarrow 255$	255
SR2	1	$R_{s,NIR}$	-	$0 \rightarrow 0.833$	$Y=0.0033*V$	$0 \rightarrow 255$	255
SR3	1	$R_{s,SWIR}$	-	$0 \rightarrow 0.625$	$Y=0.0025*V$	$0 \rightarrow 255$	255
SZA	1	Solar Zenith Angle	°	$0 \rightarrow 125$	$Y=0.500*V$	$0 \rightarrow 255$	255
VZA	1	Viewing Zenith Angle	°	$0 \rightarrow 125$	$Y=0.500*V$	$0 \rightarrow 255$	255
SAA	1	Solar Azimuth Angle	°	$0 \rightarrow 360$	$Y=1.500*V$	$0 \rightarrow 240$	255
VAA	1	Viewing Azimuth Angle	°	$0 \rightarrow 360$	$Y=1.500*V$	$0 \rightarrow 240$	255
NDV	1	NDVI	-	$-0.08 \rightarrow 0.92$	$Y=-0.08 + 0.004*V$	$0 \rightarrow 255$	255
LST	1	Land Surface Temperature	K	$223.15 \rightarrow 348.15$	$Y=-223.15 + 0.5*V$	$0 \rightarrow 255$	255
TCO	1	Clear obs.	-	$1 \rightarrow 255$	$Y=V$	$1 \rightarrow 255$	0
DAY	1	Day in Dekad	-	$1 \rightarrow 11$	$Y=V$	$1 \rightarrow 11$	0
STM	1	Status Map	-	Bit interpretation (see Table 6)		$1 \rightarrow 255$	0

With:

- DT=Datatype: 1= Byte ($V=0 \rightarrow 255$), 2 = Signed Int ($V=-32768 \rightarrow 32767$)
- $V_{lo}-V_{hi}$ =Significant V range. The scaling only holds for this range. Values beyond $V_{lo}-V_{hi}$ are flags.
- V_{flag} : Per image, only one flag indicates all "aberrant" states (sea, NoData, NoValidData, error).

The LST data layer is calculated from the channel 4 and 5 BTs (B4T and BT5), see for more details on its computation Section 3.7.

The STM (Status Map) image contains more information on the quality of the observations, as is shown in Table 6.

Table 6: Bit-interpretation of the Status Map (Bit7=Most Significant Bit, MSB).

Decimal value	128	64	32	16	8	4	2	1
Val	Bit7	Bit6	Bit5	Bit4	Bit3	Bit2	Bit1	Bit0
1	Land	Valid Obs	Never	Never	Acceptable	Cloud OR shadow	Cloud	Snow
0	Sea	No Obs	Always	Always	Good	None of these	No Cloud	No Snow

with:

- Bit7 indicates whether a pixel is land or sea/ocean. Note that ENDVI10 NDVI data are only computed for land pixels.
- As in ENDVI v1, Bit5 is unused.
- Bit4 contains information on whether the CAMS re-analysis AOT was higher than a pre-calculated maximum AOT that preserves positive RED TOC reflectances after the SMAC calculations. See for more details the ENDVI v2 ATBD. Bit4 was unused in ENDVI v1.
- No cloud shadow detection is applied, hence always Bit2 = Bit1.
- The compositing processing classifies each pixel's observation in three categories depending on the solar and viewing zenith angles: "good", "acceptable", and "bad". The last group is definitely withdrawn, but in the absence of "good" observations, "acceptable" ones may be included into the composites. This is indicated by Bit3.

Sea pixels can easily be recognised, because all bits are 0 (thus also the decimal value is zero).

5. Quality

The quality of the ENDVI v2 has been assessed for Metop-A – C for the period 2016 – 2019. The results of this validation can be found in the ENDVI v2 Validation Report (VR).

6. References

- Bartholomé E. and Belward A., "GLC2000: a new approach to global land cover mapping from Earth observation data", *Int. J. Remote Sens.*, 26, no. 9, 1959-1977 (2005).
- Berthelot B., "SMAC coefficients for METOP AVHRR/3", VEGA Technologies SAS, Toulouse, Internal report SMAC01-TN-AVHRR3-VEGA, 63 pp. (2008).
- Berthelot B., Dedieu G., Cabot F., and S. Adam, "Estimation of surface reflectances and vegetation index using NOAA/AVHRR: Methods and results at global scale", *Communications for the 6th International Symposium on Physical Measurements and Signatures in Remote Sensing*, Val d'Isère, France, Jan. 17-21, (1994).
- Coll C. and Caselles V., "A split-window algorithm for land surface temperature from Advanced Very High Resolution Radiometer data: validation and algorithm comparison", *J. Geophys. Res.*, 102 (D14), 16697-16713 (1997).
- Cracknell A., "The Advanced Very High Resolution Radiometer", Taylor & Francis, ISBN 0-7484-0209-8 (1997).
- Duveiller, G., Fasbender, D., Meroni, M., 2016a. Supplementary information for: Revisiting the concept of a symmetric index of agreement for continuous datasets. *Sci. Rep.* 6, 19401. <https://doi.org/10.1038/srep19401>
- Eerens H., Baruth B., Bydekerke L., Deronde B., Dries J., Goor E., Heyns W., Jacobs T., Ooms B., Piccard I., Royer A., Swinnen E., Timmermans A., Van Roey T., Vereecken J. & Verheijen Y., 2009, "Ten-Daily Global Composites of MetOp-AVHRR", *Proc. of the 6th International Symposium on Digital Earth*, Beijing, 9-12 September 2009.
- Eerens H., Piccard I., Royer A. and Orlandi S., 2004, "Methodology of the MARS crop yield forecasting system. Vol. 3: Remote sensing information, data processing and analysis", Eds. Royer A. and Genovese G., EUR 21291 EN/3, 76 p. (2004).
- EUMETSAT, "EPS ground segment – AVHRR L1 product generation specification", EUMETSAT, Darmstadt, Germany, Document EUM.EPS.SYS.SPE.990004, 158 pp. (2004).
- EUMETSAT, "AVHRR Level1b Products Guide", EUMETSAT, Darmstadt, Germany, Document EUM/OPS-EPS/MAN/04/0029, 123 pp. (2008).
- Inness, A., Ades, M., Agustí-Panareda, A., Barré, J., Benedictow, A., Blechschmidt, A.-M., Dominguez, J. J., Engelen, R., Eskes, H., Flemming, J., Huijnen, V., Jones, L., Kipling, Z., Massart, S., Parrington, M., Peuch, V.-H., Razinger, M., Remy, S., Schulz, M., and Suttie, M., "The CAMS reanalysis of atmospheric composition", *Atmos. Chem. Phys.*, 19, 3515–3556, <https://doi.org/10.5194/acp-19-3515-2019>, 2019.
- Rahman H. and Dedieu G., "SMAC: a Simplified Method for the Atmospheric Correction of Satellite Measurements in the Solar Spectrum", *Int. J. Remote Sens.*, 15(1), 123-143 (1994).
- Swinnen, E., Dierckx, W., "Validation Report - Normalized Difference Vegetation Index". SAF/LAND/VITO/VR_endvi/2.0. (2015)
- Wu, X., Naegeli, K., Wunderle, S., "Geometric accuracy assessment of global coarse resolution satellite data sets: a study based on AVHRR GAC data at the subpixel level". *Earth Syst. Sci. Data Discuss.* In review, 1–22. <https://doi.org/10.5194/essd-2019-87> (2019)

Acknowledgements

The development and implementation have been originally carried out in the JRC-MARS program under the responsibility of the institutes VITO-TAP and JRC-IPSC with support of the Belgian Science Policy Office (BELSPO). The global operations and improvements are further carried out under the responsibility of EUMETSAT's LSA SAF program.